

*Journal of the American Chemical Society*

## **Supporting Information**

### **H-Bonded Supramolecular Polymer for the Selective Dispersion and Subsequent Release of Large-Diameter Semiconducting Single- Walled Carbon Nanotubes**

*Igor Pochorovski, Huiliang Wang, Jeremy I. Feldblyum, Xiaodong Zhang, Alexander L.  
Antaris, and Zhenan Bao\**

# Table of Contents

<b>1. SYNTHESIS SECTION</b>	<b>3</b>
1.1. Synthetic efforts towards an alternative supramolecular polymer	3
1.2. Synthesis of compound 1	3
1.3. Materials and general methods	4
1.4. Synthetic procedures	4
1.5. NMR Spectra of the Products	7
<b>2. CORRELATION BETWEEN DOSY DIFFUSION COEFFICIENT AND POLYMER 1 MOLECULAR WEIGHT</b>	<b>10</b>
<b>3. DISPERSION EXPERIMENTS</b>	<b>11</b>
3.1. Experimental procedure	11
3.2. Determination of the SWNT content in the SWNT sample (P2-SWNTs)	12
3.3. Determination of the extinction coefficient and yield of dispersed SWNTs	12
3.4. Influence of dispersion conditions on SWNT dispersion yield and purity	13
3.5. Comparison of the dispersion properties of polymer 1	15
<b>4. CHARACTERIZATION OF SWNT DISPERSIONS</b>	<b>17</b>
4.1. Absorption spectroscopy	17
4.2. Raman Spectroscopy	17
4.3. Photoluminescence vs. Excitation (PLE) Mapping	17
4.4. X-ray photoelectron spectroscopy (XPS)	18
<b>5. REFERENCES</b>	<b>19</b>

## 1. Synthesis section

### 1.1. Synthetic efforts towards an alternative supramolecular polymer

Supramolecular polymer **4** was also targeted in addition to **1** and contains an alkyne unit as a linker between the fluorene and the UPy unit. Retrosynthetic routes A (involving iodo-UPy **5** and diethynyl-fluorene **6**) and B (involving alkynyl-UPy **7** and the diiodo-fluorene **8**) both featuring Sonogashira coupling<sup>1</sup> (Figure S1) were explored. However, we found that compounds of that type are unstable, as rearrangement of compound **9** to **10** was observed.

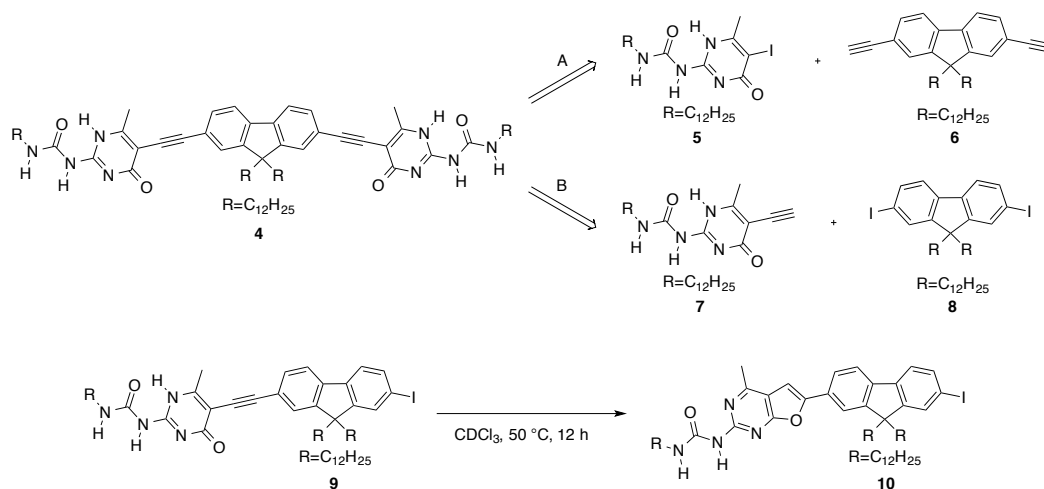


Figure S1. Alternative supramolecular polymer **4**.

### 1.2. Synthesis of compound **1**

The synthesis of target compound **1** required preparation of precursor vinyl-UPy **2**, which was accessed in two steps from iodocytosine **11** (Figure S2). In the first step, compound **11** was reacted with dodecyl isocyanate to yield iodo-UPy **5** using a literature procedure.<sup>1</sup> In the second step, compound **5** was converted into vinyl-UPy **2** via Stille coupling with tributyl(vinyl)stannane.

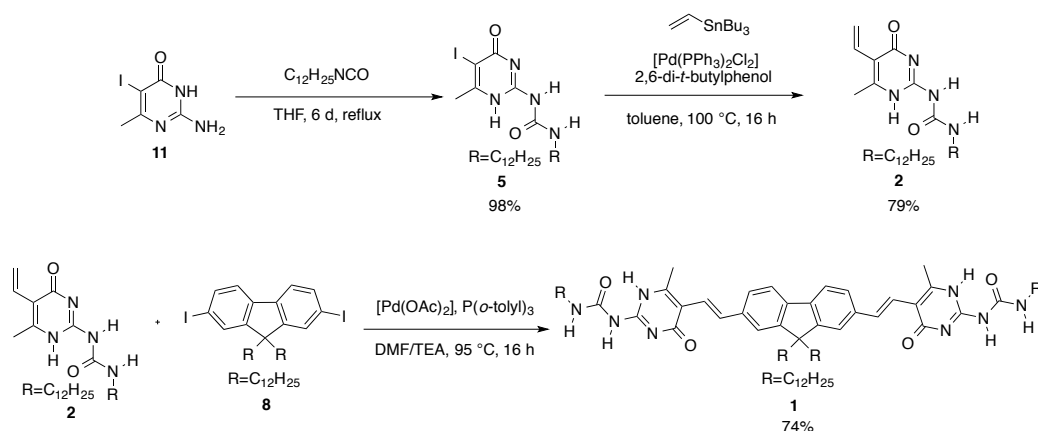


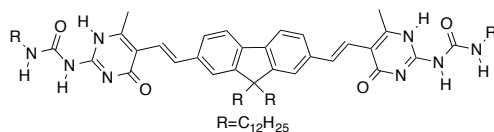
Figure S2. Synthesis of compound 1.

### 1.3. Materials and general methods

All chemicals were purchased as reagent grade from commercial sources and used without further purification. When stated, solvents were degassed by bubbling  $N_2$  through the solution for 30 min.  $^1H$  NMR and  $^{13}C$  NMR spectra were recorded on a Mercury 400 or Inova 600 spectrometer at 298 K. Residual solvent peaks were used as internal references. High-resolution electrospray ionization mass spectra were measured by direct injection on the Bruker MicroTOF-Q II time of flight mass spectrometer with Agilent 1260 HPLC at the Vincent Coates Foundation Mass Spectrometry Laboratory, Stanford University Mass Spectrometry. Data was collected in positive ion mode with a mass range of 50-1200 Da. High-resolution matrix-assisted laser-desorption-ionization mass spectra were measured on a Bruker Daltonics Ultraflex II MALDI-TOF mass spectrometer using (2-[(2*E*)-3-(4-*t*-butylphenyl)-2-methylprop-2-enylidene]malononitrile) (DCTB) as matrix by the MS-service at ETH Zürich.

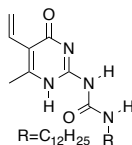
### 1.4. Synthetic procedures

Compounds **3**,<sup>2</sup> **5**,<sup>3</sup> and **12**<sup>4</sup> were prepared according to literature procedures. Poly(9,9-di-*n*-dodecylfluorene) (PFDD) was purchased from Sigma-Aldrich.



**1,1'-(((1*E*,1'*E*)-(9,9-didodecyl-9H-fluorene-2,7-diyl)bis(ethene-2,1-diyl))bis(6-methyl-4-oxo-1,4-dihydropyrimidine-5,2-diyl))bis(3-dodecylurea) (1)**

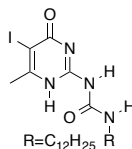
UPy compound **2** (1.7 g, 4.7 mmol) and diiodofluorene **8** (1.6 g, 2.1 mmol) were suspended in a mixture of DMF (100 mL) and TEA (30 mL) under N<sub>2</sub> atmosphere. The mixture was degassed and [Pd(AOc)<sub>2</sub>] (48 mg, 0.21 mmol) and tri(*o*-tolyl)phosphine (130 mg, 0.42 mmol) were added. The mixture was stirred at 95 °C for 16 h, then filtered hot over glass wool. The bright orange solution was concentrated *in vacuo*. The remaining solid was dissolved in CHCl<sub>3</sub> (70 mL)/TFA (1 mL) and precipitated with MeOH (120 mL). The precipitate was filtered off and washed with MeOH. This reprecipitation procedure was repeated two more times to afford compound **1** (1.9 g, 74%) as a yellow solid. Compound **1** dissolves very slowly in chloroform and is only sparingly soluble in toluene, but rapidly dissolves upon addition of small quantities of trifluoroacetic acid (TFA) in both solvents. <sup>1</sup>H NMR (600 MHz, CDCl<sub>3</sub>): δ = 0.53 – 0.74 (m, 4H), 0.86 (dt, *J* = 13.1, 7.0, 12H), 0.96 – 1.54 (m, 72H), 1.72 (s, 4H), 1.95 (d, *J* = 31.6, 4H), 2.49 (s, 6H), 3.33 (s, 4H), 6.98 (d, *J* = 16.4, 2H), 7.40 (s, 2H), 7.47 (s, 2H), 7.64 (d, *J* = 8.3, 2H), 7.81 (d, *J* = 14.9, 2H), 10.29 (s, 2H), 11.96 (s, 2H), 13.25 ppm (s, 2H). <sup>13</sup>C NMR (151 MHz, CDCl<sub>3</sub>): δ = 14.4, 18.4, 24.1, 27.3, 29.4, 29.6, 29.6, 29.7, 29.9, 29.9, 29.9, 30.0, 30.4, 32.1, 32.2, 40.4, 55.2, 115.0, 119.1, 120.0, 121.2, 125.7, 134.6, 137.2, 140.9, 144.2, 151.7, 152.6, 157.0, 171.3 ppm. HR-MALDI-MS (DCTB): *m/z* (%): 1223.9633 (100, [*M*+H]<sup>+</sup>, calcd for C<sub>77</sub>H<sub>123</sub>N<sub>8</sub>O<sub>4</sub><sup>+</sup>: 1223.9667).



### 1-Dodecyl-3-(6-methyl-4-oxo-5-vinyl-1,4-dihydropyrimidin-2-yl)urea (**2**)

Compound **5** (4.0 g, 8.7 mmol), [Pd(PPh<sub>3</sub>)<sub>2</sub>Cl<sub>2</sub>] (304 mg, 433 mmol), and 2,6-di-*t*-butylphenol (37 mg, 0.17 mmol) were dissolved in toluene (60 mL). Tributyl(vinyl)stannane (3.0 mL, 10 mmol) was added. The mixture was degassed and heated to 100 °C for 16 h. The mixture was filtered hot over a plug of cotton followed by hot filtration over Celite. The obtained yellow-orange solution was cooled to 25 °C, resulting in crystal formation. The formed crystals were filtered off, washed with small quantities of toluene, and dried, to afford compound **2** as a white solid (2.49 g, 79%). <sup>1</sup>H NMR (400 MHz, CDCl<sub>3</sub>): δ = 0.85 – 0.91 (m, 3H), 1.25 (s, 18H), 1.53 – 1.73 (m, 2H), 2.34 (s, 3H), 3.25 (td, *J* = 7.2, 5.3, 2H), 5.46 (dd, *J* = 11.7, 2.2, 1H), 6.09 (dd, *J* = 17.6, 2.2, 1H), 6.53 (dd, *J* = 17.6, 11.7, 1H), 10.18 (s, 1H), 11.86 (s, 1H), 13.12 ppm (s, 1H).

$^{13}\text{C}$  NMR (151 MHz,  $\text{CDCl}_3$ ):  $\delta$  = 14.3, 18.0, 22.9, 27.3, 29.4, 29.6, 29.8, 29.9, 29.9, 32.1, 40.4, 114.9, 119.9, 128.0, 144.4, 152.9, 156.9, 171.3 ppm. HR-ESI-MS:  $m/z$  (%): 363.2748 (100,  $[M+H]^+$ , calcd for  $\text{C}_{20}\text{H}_{35}\text{N}_4\text{O}_2^+$ : 363.2755).



### 1-Dodecyl-3-(5-iodo-6-methyl-4-oxo-1,4-dihydropyrimidin-2-yl)urea (**5**)

2-Amino-5-iodo-6-methylpyrimidin-4(3*H*)-one (**11**) (12.4 g, 49.4 mmol) was suspended in dry THF (500 mL). Dodecyl isocyanate (20.2 mL, 84.0 mmol) was added, and the mixture was stirred at 90 °C for 8 d. The mixture was cooled to 25 °C, the formed precipitate was filtered off, and washed with  $\text{CH}_2\text{Cl}_2$  to afford compound **5** as a white solid (22.0 g, 96%).  $^1\text{H}$  NMR (600 MHz,  $\text{CDCl}_3$ ):  $\delta$  = 0.87 (t,  $J$  = 7.0, 3H), 1.17 – 1.40 (m, 18H), 1.59 (q,  $J$  = 7.2, 2H), 2.47 (s, 3H), 3.24 (q,  $J$  = 6.6, 2H), 9.83 (s, 1H), 11.60 (s, 1H), 13.41 ppm (s, 1H).  $^{13}\text{C}$  NMR (151 MHz,  $\text{CDCl}_3$ ):  $\delta$  = 14.3, 22.9, 25.5, 27.2, 29.4, 29.6, 29.9, 29.9, 29.9, 32.2, 40.5, 82.6, 150.5, 154.3, 156.5, 169.4 ppm. HR-ESI-MS:  $m/z$  (%): 485.1361 (100,  $[M+\text{Na}]^+$ , calcd for  $\text{C}_{18}\text{H}_{30}\text{IN}_4\text{O}_2\text{Na}^+$ : 485.1378).

## 1.5. NMR Spectra of the Products

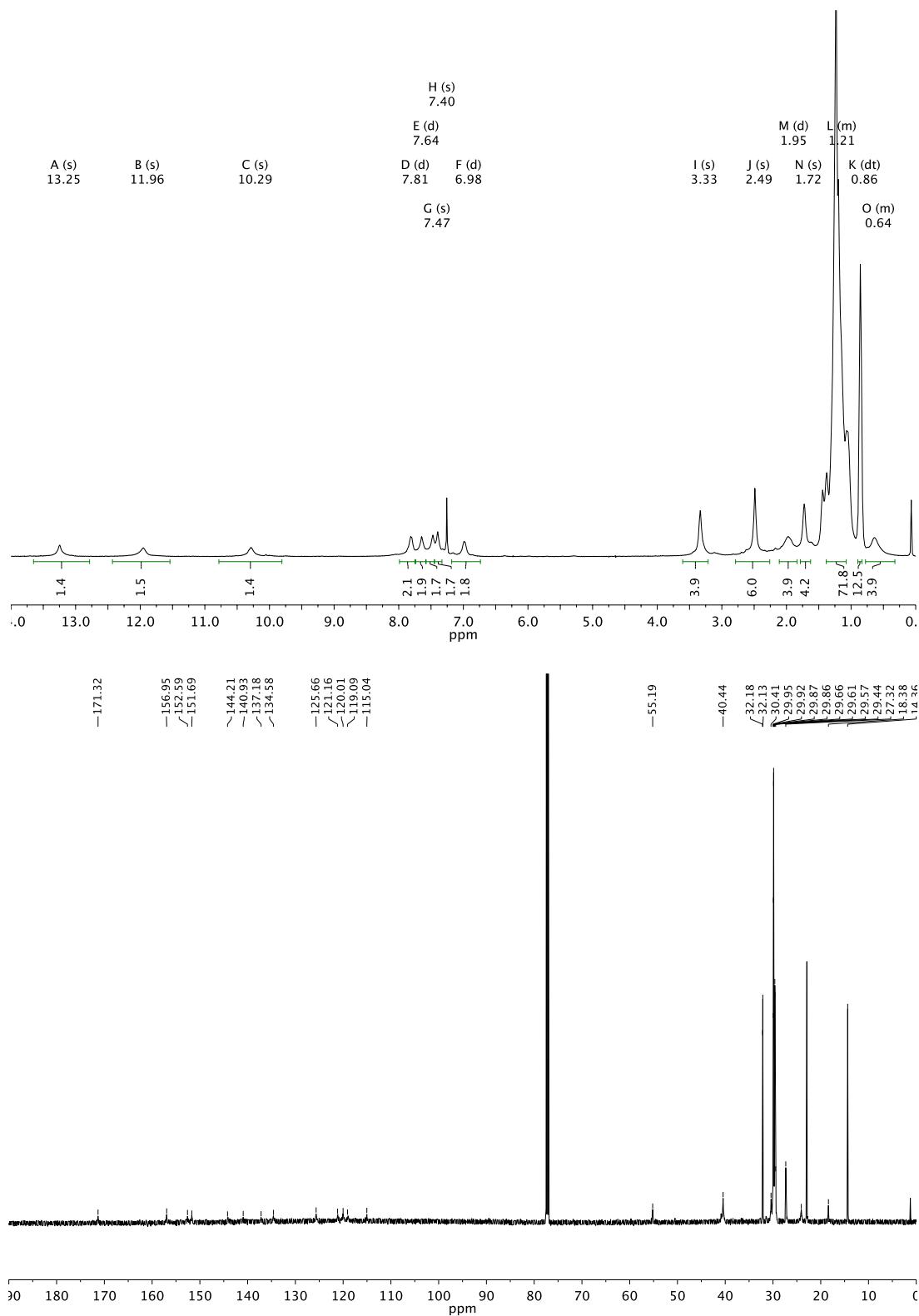


Figure S3.  $^1\text{H}$  NMR (top, 600 MHz) and  $^{13}\text{C}$  NMR (bottom, 151 MHz) spectra of compound **1** in  $\text{CDCl}_3$  at 298 K.

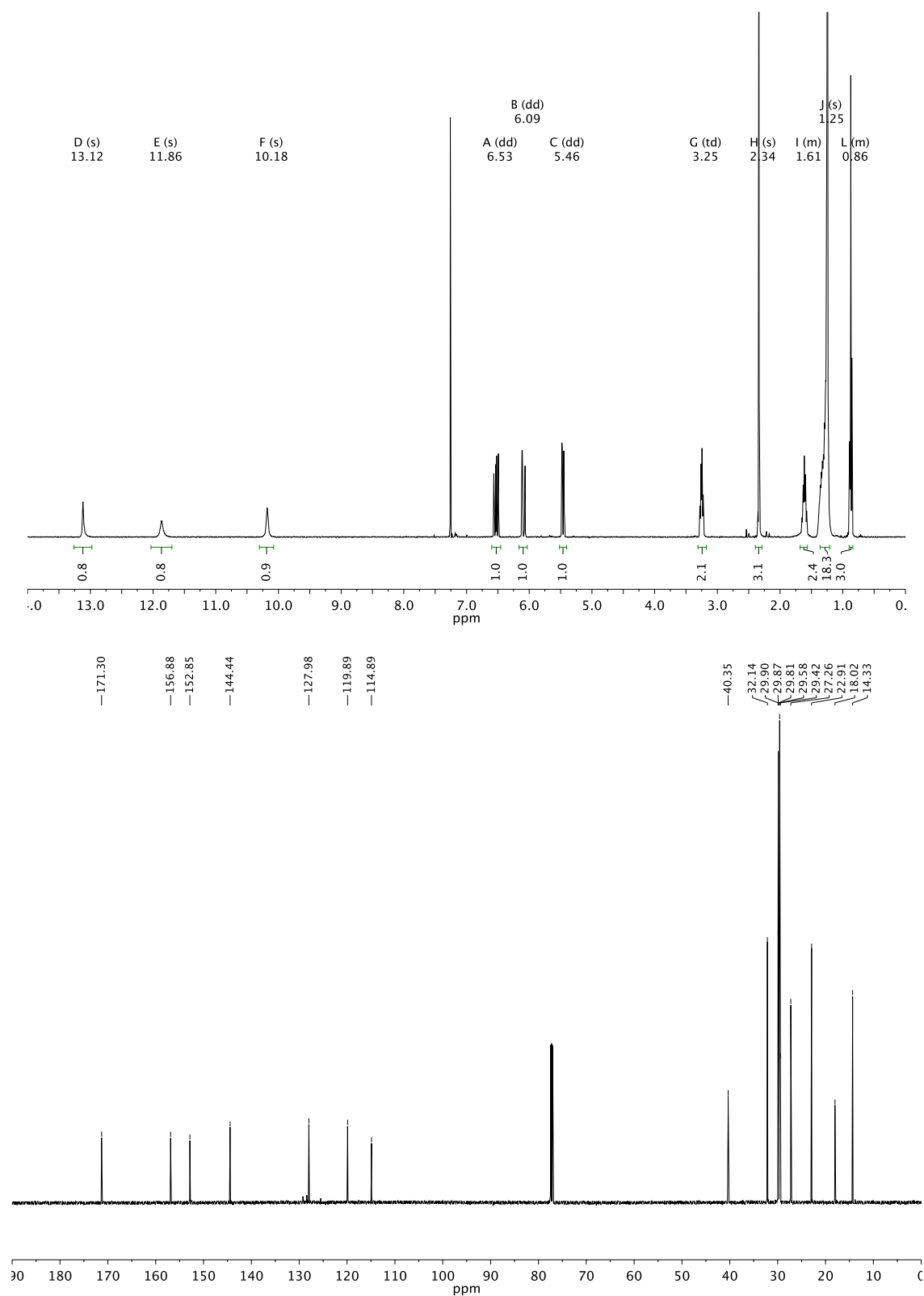


Figure S4. <sup>1</sup>H NMR (top, 400 MHz) and <sup>13</sup>C NMR (bottom, 151 MHz) spectra of compound **2** in CDCl<sub>3</sub> at 298 K.



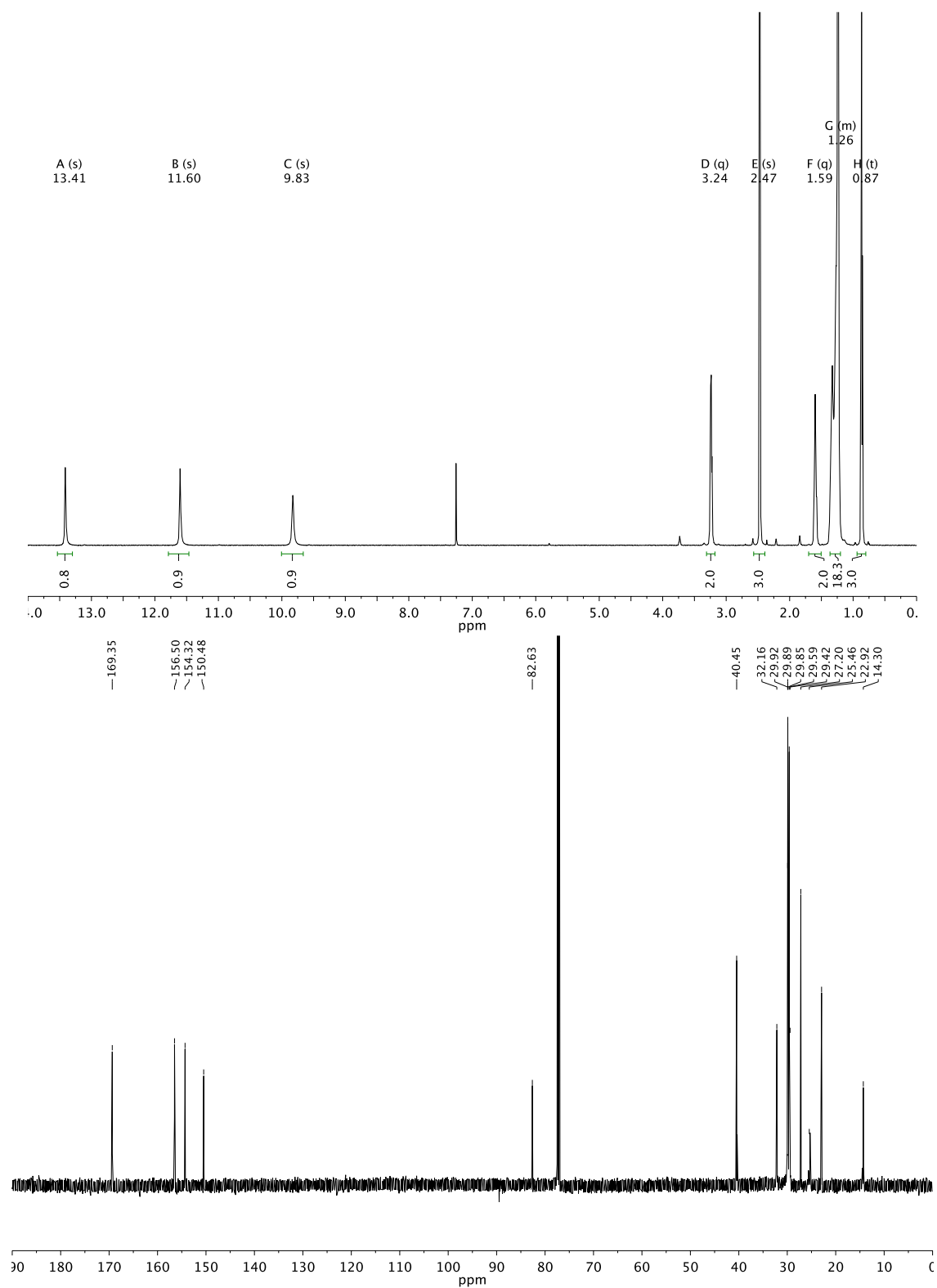


Figure S5. <sup>1</sup>H NMR (top, 600 MHz) and <sup>13</sup>C NMR (bottom, 151 MHz) spectra of compound **5** in CDCl<sub>3</sub> at 298 K.

## 2. Correlation between DOSY diffusion coefficient and polymer 1 molecular weight

A titration study of supramolecular polymer **1** with monofunctional chain stopper **2** allowed us to relate the relative diffusion coefficient of polymer **1** to its molecular weight (Figure S6A). We utilized the fact that at sufficiently high molar fractions  $x$  of the chain stopper **2**, the degree of polymerization  $N$  can be described by the simple relation:<sup>5</sup>

$$N = 2/x$$

On the other hand, the average molecular weight  $M$  as a function of  $N$  is

$$M = (N-1) \times M(1) + 2 \times M(2)$$

as a given  $N$  represents a linear chain of  $N-1$  monomers **1** end-capped by two monofunctional chains stoppers **2**. Assuming the exponential relation between  $D$  and  $M$

$$D = p \times M^q$$

plotting

$$\log D = \log p + q \log M$$

should yield a straight line with slope  $q$  and  $y$ -intercept  $\log p$ . Figure S6B shows this plot together with the extracted parameters  $\log p$  and  $q$ , which were utilized to calculate  $M$  and  $N$  of polymer **1** as a function of its concentration (Figure S6C, compare with Figure 2A in the manuscript).

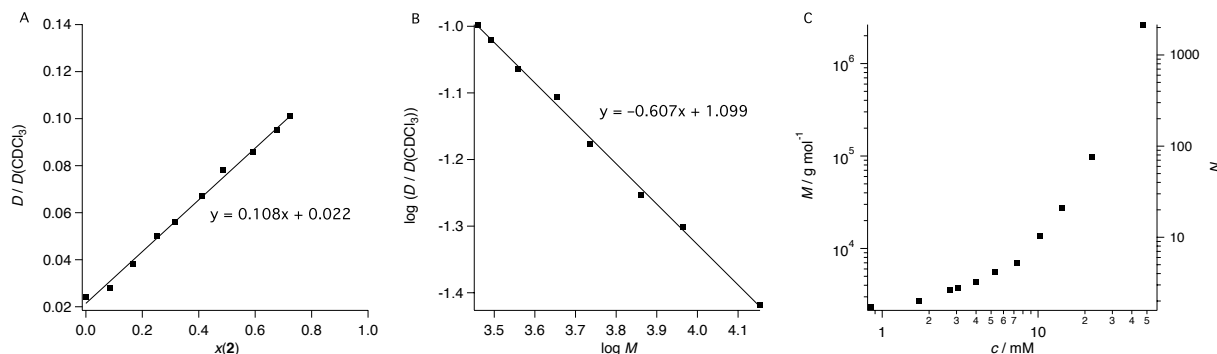


Figure S6. A) Relative diffusion coefficient of bifunctional compound **1** as a function of added molar fraction  $x$  of monofunctional chain stopper **2**. B) Measured relative diffusion coefficients vs. calculated molecular weights. C) Molecular weight  $M$  and degree of polymerization  $N$  of compound **1** as a function of concentration.

### 3. Dispersion experiments

The general procedure for a dispersion experiment is described in Section 3.1. We investigated the influence of various dispersion parameters, including polymer **1**/SWNT ratio, SWNT concentration, sonication power, and sonication time on the yield and purity of the obtained SWNT dispersions. We define the SWNT dispersion yield as the mass percentage of dispersed SWNTs relative to the mass of SWNTs present in the employed SWNT sample. In addition to actual SWNTs, a SWNT sample usually contains metal catalyst, amorphous carbon, and graphitic impurities. Therefore, knowledge of the actual SWNT content in the employed SWNT sample (P2-SWNTs) is required to obtain SWNT dispersion yields. The determination of the SWNT content is described in Section 3.2. Because polymer **1** can be removed from the dispersed SWNTs, we were able for the first time to directly quantify the SWNT dispersion yield by measuring the mass of released SWNTs. We performed this procedure once with dispersion conditions that yielded a relatively large amount of dispersed SWNTs in order to reduce the weighing error. We then used the obtained mass yield together with absorption spectroscopy data to calculate SWNT dispersion yields for other dispersion conditions. This procedure is described in Section 3.3. While absolute quantification of the sc/met-SWNT ratio via absorption spectroscopy is not possible, the  $\phi$  value has recently been proposed as a relative measure for the sc-SWNT purity.<sup>6</sup> The procedure for obtaining  $\phi$  values from absorption spectroscopy data is described in detail in the Supporting Information of that work.<sup>6</sup> The results of the study of dispersion conditions on SWNT dispersion yield and purity are summarized in Section 3.4

#### 3.1. Experimental procedure

Dispersion experiments were performed using a Cole Parmer – CP 750 Ultrasonicator with a 0.7 cm sonication tip on polymer **1**/SWNT samples in toluene. For a typical dispersion experiment, polymer and SWNTs were combined in a test tube, 20 mL toluene was added, and the mixture was sonicated for a given time at a given sonication power. The test tube was cooled using an external circulator with a bath temperature set to 22 °C. The sonicated samples were then centrifuged for 30 min at 17000 rpm and 16 °C, the supernatants carefully removed with a syringe, and analyzed by absorption spectroscopy.

### 3.2. Determination of the SWNT content in the SWNT sample (P2-SWNTs)

The actual content of SWNTs in the employed SWNT sample can be determined using TGA analysis or absorption spectroscopy, as described in prior studies.<sup>6-7</sup> For laser vaporization<sup>7a</sup> and plasma-derived<sup>6</sup> SWNTs, this content was determined to be 33% and 53%, respectively. For the P2-SWNTs employed in this study, the manufacturer (Carbon Solutions, Inc.) kindly provided us with the analytical data for our batch (Lot 02-A007 CO 1763). According to near-IR analysis (Figure S7, left) the SWNT fraction in the sample is ~70%, while graphitic nanoparticles correspond to the remaining 30% of the total nanocarbon content. According to TGA analysis, the residual catalyst impurities contribute to 7% of the overall SWNT sample mass (Figure S7, right). From these data, the SWNT content in the SWNT sample can be calculated to be 65%.

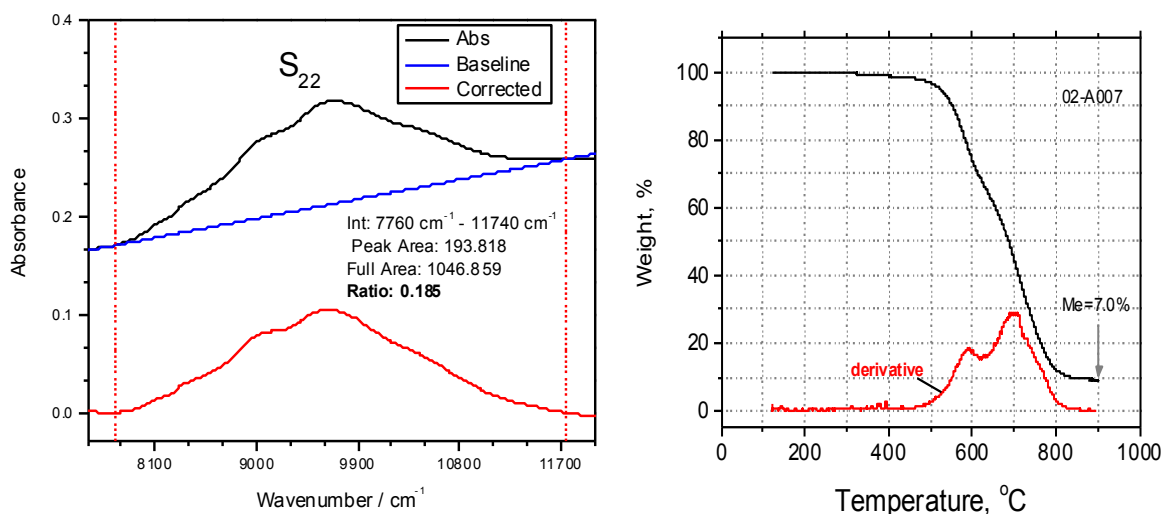


Figure S7. Near-IR (left) and TGA analysis (right) of P2-SWNTs (Lot 02-A007 CO 1763) provided by Carbon Solutions, Inc.

### 3.3. Determination of the extinction coefficient and yield of dispersed SWNTs

Polymer **1** (26.6 mg) and AD-SWNTs (26.0 mg) were sonicated in 20 mL toluene for 30 min at 70% power while externally cooled with a water circulator set to 22 °C. The mixture was centrifuged for 30 min at 17000 and 16 °C. Absorption spectroscopy revealed a peak absorption of  $A = 0.312$  at  $\lambda = 1016$  nm for a  $d = 0.1$  cm cuvette. 15 mL of this solution were treated with 0.15 mL TFA, resulting in SWNT precipitation. The SWNTs were filtered over a 0.2  $\mu$ L PTFE membrane (whose mass was prior determined with a microbalance), washed with 20 mL TFA solution (1% in toluene), then with 10 mL toluene, and dried in air. Weighing the PTFE membrane with the SWNTs yielded a SWNT mass of 0.90 mg, which scales to 1.20 mg in the

original 20 mL dispersion. These data correspond to an extinction coefficient of  $\varepsilon = 52 \text{ mL mg}^{-1} \text{ cm}^{-1}$  according to the Lambert-Beer law ( $A = \varepsilon cd$ ), which is similar to the recently reported value of  $\varepsilon = 48.3 \text{ mL mg}^{-1} \text{ cm}^{-1}$  determined using an indirect approach.<sup>6</sup> Assuming a SWNT content of 65% (derived in Section 3.2) in the original SWNT sample, the SWNT dispersion yield of that sample amounts to 7.1%. With that information, the SWNT dispersion yields obtained with other dispersion conditions were calculated from the respective absorption maxima at  $\lambda = 1016 \text{ nm}$ .

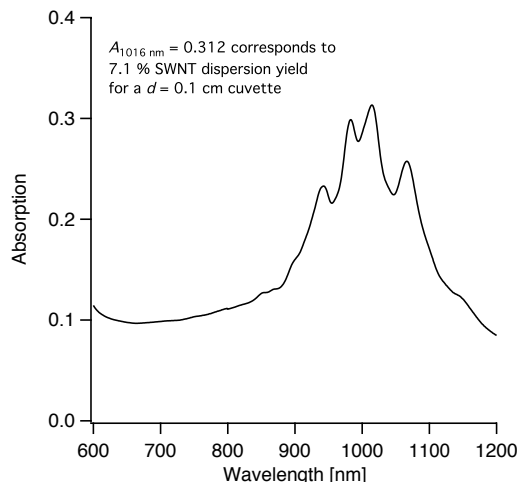


Figure S8. Absorption spectrum for a SWNT dispersion obtained from sonicating polymer **1** (26.6 mg) and AD-SWNTs (26.0 mg) in 20 mL toluene for 30 min at 70% power.

### 3.4. Influence of dispersion conditions on SWNT dispersion yield and purity

We found that both SWNT dispersion yield and sc-SWNT purity first increase with increasing polymer **1**/SWNT ratio, but then level out at a ratio of ca. 1.5 (Figure S9). On the other hand, while the SWNT dispersion yield decreases with increasing input SWNT concentration  $w(\text{SWNT})$ , the sc-SWNT purity slightly increases (Figure S10). Finally, lower sonication powers or times lead to lower SWNT yields but significantly higher sc-SWNT purities (Figure S11 and S12).

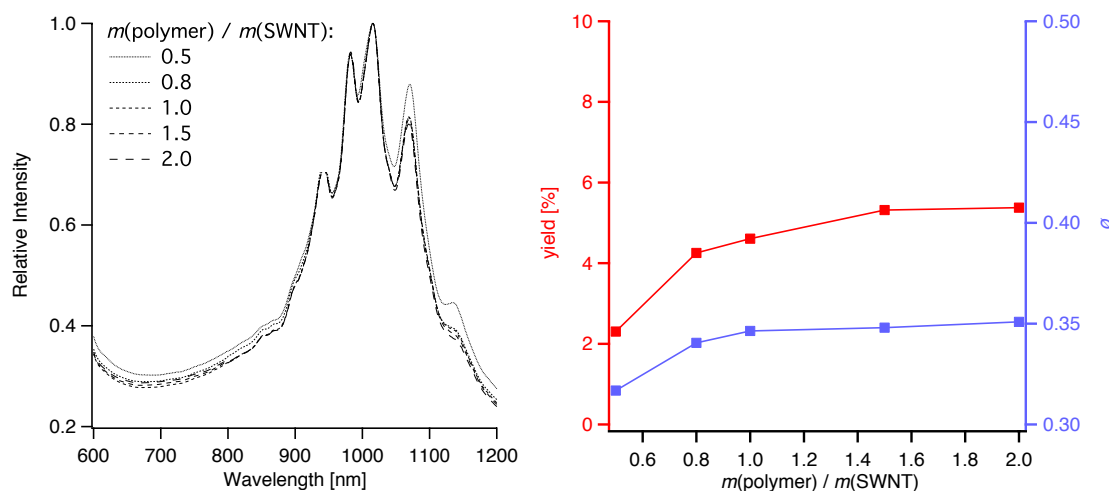


Figure S9. Influence of  $m(\text{polymer } 1)/m(\text{SWNT})$  ratio on SWNT dispersion yield and purity. Left: absorption spectra of dispersions utilizing various  $m(\text{polymer } 1)/m(\text{SWNT})$  ratios with  $m(\text{SWNT}) = 5 \text{ mg}$  (30 min sonication at 40% power). The spectra were normalized for the maximum at 1016 nm. Right: plot showing the SWNT dispersion yields and  $\phi$  values extracted from the absorption spectra showed on the left.

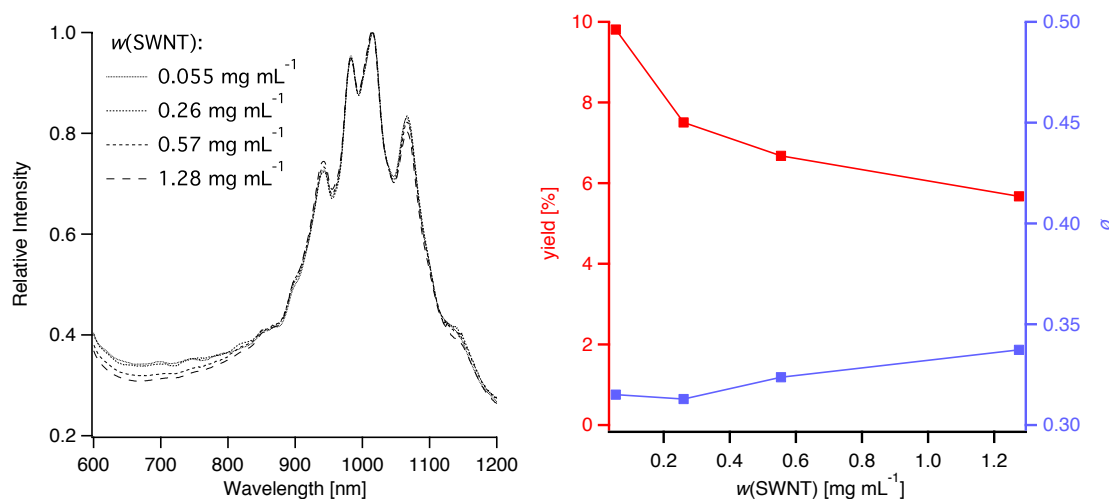


Figure S10. Influence of the initial SWNT concentration  $w(\text{SWNT})$  on SWNT dispersion yield and purity. Left: absorption spectra of dispersions utilizing various  $w(\text{SWNT})$  with  $m(\text{polymer } 1)/m(\text{SWNT}) = 1.0$  (30 min sonication at 70% power). The spectra were normalized for the maximum at 1016 nm. Right: plot showing the SWNT dispersion yields and  $\phi$  values extracted from the absorption spectra showed on the left.

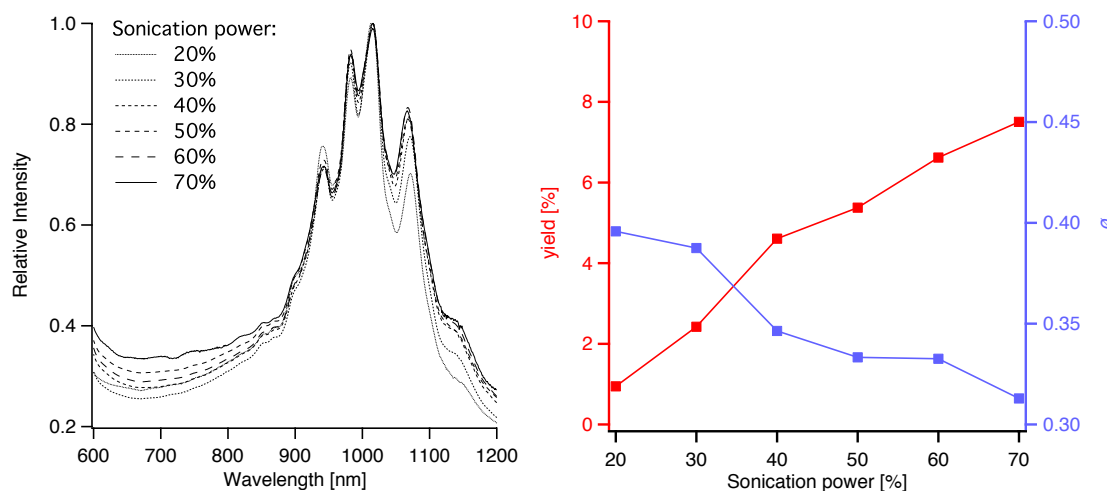


Figure S11. Influence of sonication power on SWNT dispersion yield and purity. Left: absorption spectra of dispersions utilizing various sonication powers with  $m(\text{SWNT}) = 5 \text{ mg}$  and  $m(\text{polymer } 1)/m(\text{SWNT}) = 1.0$  (30 min sonication). The spectra were normalized for the maximum at 1016 nm. Right: plot showing the SWNT dispersion yields and  $\phi$  values extracted from the absorption spectra showed on the left.

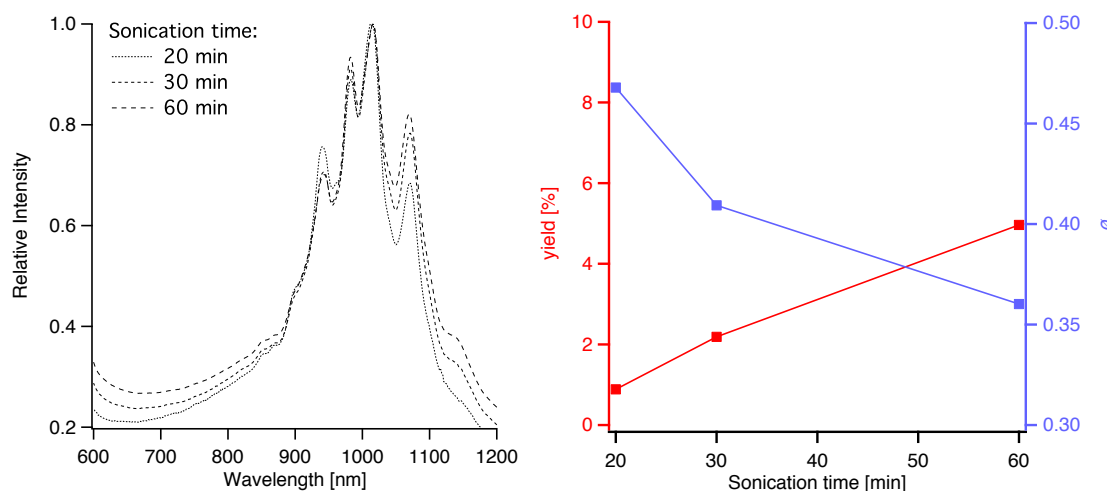


Figure S12. Influence of sonication time on SWNT dispersion yield and purity. Left: absorption spectra of dispersions utilizing various sonication times with  $m(\text{SWNT}) = 5 \text{ mg}$  and  $m(\text{polymer } 1)/m(\text{SWNT}) = 1.0$  (30 % sonication power). The spectra were normalized for the maximum at 1016 nm. Right: plot showing the SWNT dispersion yields and  $\phi$  values extracted from the absorption spectra showed on the left.

### 3.5. Comparison of the dispersion properties of polymer 1

The ability of polymer 1 to disperse SWNTs was compared with the corresponding conventional polymer poly(9,9-di-*n*-dodecylfluorene) (PFDD) and monofunctional UPy compound 2 (Figure S13) under the same dispersion conditions (5 mg dispersing agent, 5 mg AD-SWNTs, 30 min sonication at 70% power). Polymer 1 exhibited a ca. 7 times higher dispersion yield and higher purity ( $\phi = 0.31$  for polymer 1 vs.  $\phi = 0.27$  for PDDD). UPy compound 2 showed no ability to disperse SWNTs.

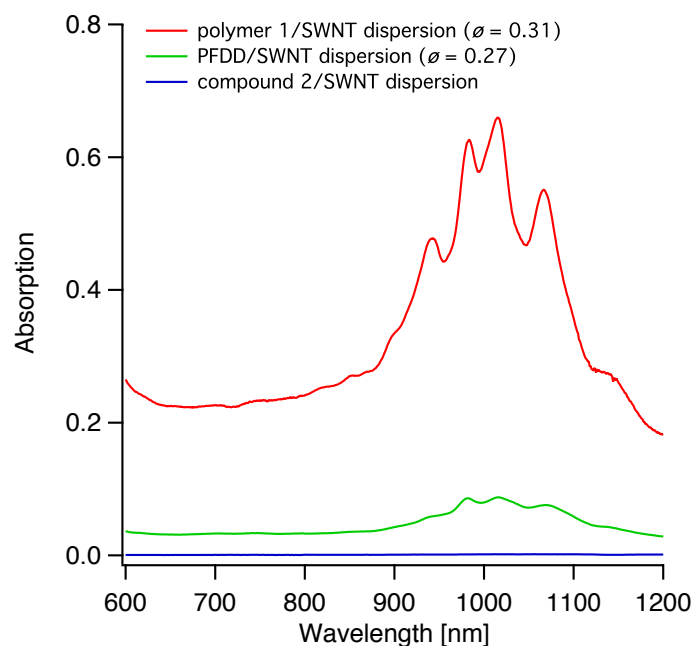


Figure S13. Absorption spectra of SWNT dispersions obtained using polymer **1**, poly(9,9-di-*n*-dodecylfluorene) (PFDD), and monofunctional UPy compound **2** as dispersing agents under the same dispersion conditions (5 mg dispersing agent, 5 mg AD-SWNTs, 30 min sonication at 70% power).

We also compare a polymer **1**/SWNT sample obtained under dispersion conditions optimized for a high purity (5 mg polymer **1**, 5 mg AD-SWNTs, 20 min sonication at 30% power) with a commercial polymer/SWNT sample from NanoIntegris<sup>8</sup> (Figure S14). This comparison is directed at the maximum achievable SWNT purity.

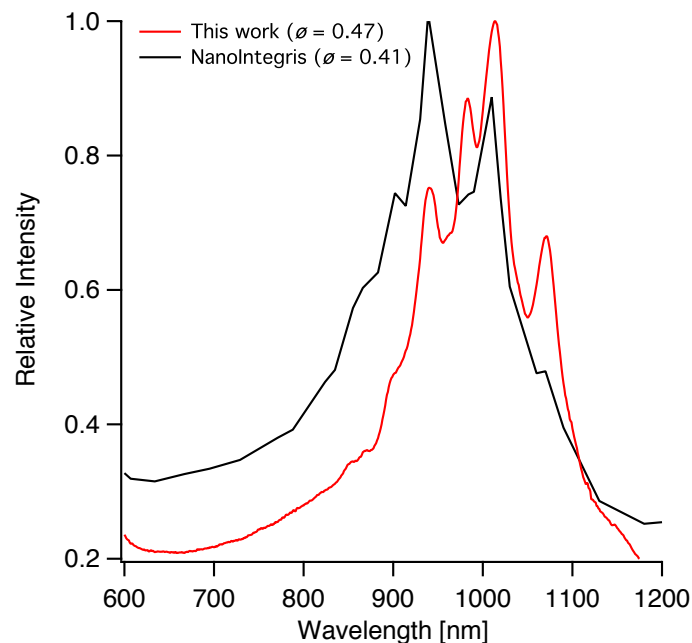


Figure S14. Absorption spectra of a polymer **1**/SWNT sample (5 mg polymer **1**, 5 mg AD-SWNTs, 20 min sonication at 30% power) and of a polymer/SWNT sample from NanoIntegris (latter spectrum taken from website).<sup>8</sup>



## 4. Characterization of SWNT dispersions

### 4.1. Absorption spectroscopy

Absorption spectroscopy was carried out on an Agilent Cary 6000i (Agilent Technologies, Santa Clara, CA).

### 4.2. Raman Spectroscopy

Raman spectra were recorded on a confocal Raman microscope (Horiba XploRa One) at 532 nm, 638 nm, and 785 nm excitation at 100x magnification. The sorted SWNT sample was prepared by drop-casting a polymer 1/SWNT solution (sorted SWNTs) on a Si substrate. The as-received AD-SWNT sample was prepared by drop-casting an AD-SWNT dispersion in NMP on a Si substrate. The dispersion was obtained by sonicating 1.7 mg AD-SWNTs in 20 mL NMP for 30 min at 70% sonication power, followed by centrifugation at 16000 rpm for 30 min. Data were processed by averaging 9 spectra measured at different locations. Characteristic regions of the Raman spectra are showed in Figure S15.

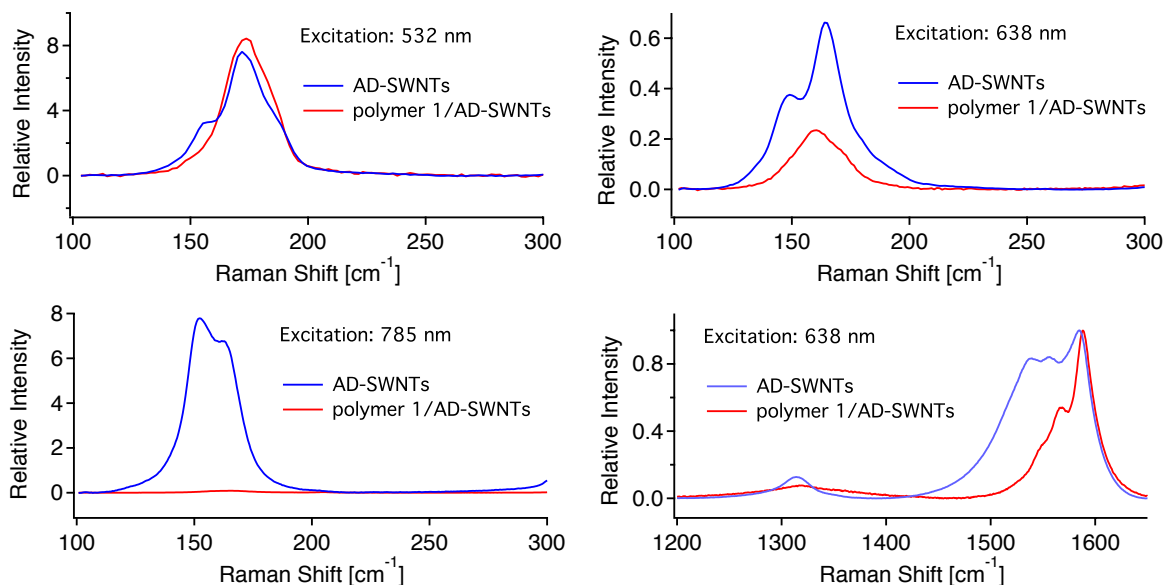


Figure S15. Comparison of Raman spectra of as-received and sorted AD-SWNTs at various excitation wavelengths.

### 4.3. Photoluminescence vs. Excitation (PLE) Mapping

PLE spectra were measured on a home-built NIR spectroscopy setup in the region of 1150-2100 nm. The excitation source was a 150 W ozone-free Xenon lamp (Oriel), whose light was

dispersed by a monochromator (Oriel) to generate excitation lines with a bandwidth of 15 nm. The excitation light in the range of 700-1050 nm was focused on the sample and filtered by a 1100-nm short-pass filter (Thorlabs). The emission was collected in the 1150-2100 nm emission range using a 1100-nm long-pass filter. The emission was collected with a spectrometer (Acton SP2300i) equipped with a liquid-nitrogen-cooled InGaAs 1-dimensional detector (Princeton OMA-V). PLE data were plotted post-collection to account for the sensitivity of the detector, extinction features of the filter, and the power of the excitation using MATLAB.

#### **4.4. X-ray photoelectron spectroscopy (XPS)**

Samples were analyzed with a PHI Versaprobe Scanning XPS (Physical Electronics, Chanhassen, MN) having a Al K $\alpha$  source with a monochromator. A pressure of  $< 1 \times 10^{-8}$  Torr was achieved before measurement, and neutralizer was used during data collection.

## 5. References

- (1) (a) Wang, X.-Z.; Li, X.-Q.; Shao, X.-B.; Zhao, X.; Deng, P.; Jiang, X.-K.; Li, Z.-T.; Chen, Y.-Q., *Chem. Eur. J.* **2003**, *9*, 2904; (b) Li, X.-Q.; Jia, M.-X.; Wang, X.-Z.; Jiang, X.-K.; Li, Z.-T.; Chen, G.-J.; Yu, Y.-H., *Tetrahedron* **2005**, *61*, 9600.
- (2) Maji, M. S.; Pfeifer, T.; Studer, A., *Chem. Eur. J.* **2010**, *16*, 5872.
- (3) Lee, S. H.; Nakamura, T.; Tsutsui, T., *Org. Lett.* **2001**, *3*, 2005.
- (4) Wierenga, W.; Skulnick, H. I.; Stringfellow, D. A.; Weed, S. D.; Renis, H. E.; Eidson, E. E., *J. Med. Chem.* **1980**, *23*, 237.
- (5) (a) Knoben, W.; Besseling, N. A. M.; Cohen Stuart, M. A., *Macromolecules* **2006**, *39*, 2643; (b) Lortie, F.; Boileau, S.; Bouteiller, L.; Chassenieux, C.; Lauprêtre, F., *Macromolecules* **2005**, *38*, 5283.
- (6) Ding, J.; Li, Z.; Lefebvre, J.; Cheng, F.; Dubey, G.; Zou, S.; Finnie, P.; Hrdina, A.; Scoles, L.; Lopinski, G. P.; Kingston, C. T.; Simard, B.; Malenfant, P. R. L., *Nanoscale* **2014**, *6*, 2328.
- (7) (a) Mistry, K. S.; Larsen, B. A.; Blackburn, J. L., *Acs Nano* **2013**, *7*, 2231; (b) Itkis, M. E.; Perea, D. E.; Jung, R.; Niyogi, S.; Haddon, R. C., *J. Am. Chem. Soc.* **2005**, *127*, 3439.
- (8) IsoSol-S100® Polymer-Wrapped Nanotubes from NanoIntegris.  
<http://www.nanointegris.com/en/IsoSol-S100>.